THE JOURNAL OF BIOLOGICAL CHEMISTRY VOL. 289, NO. 15, pp. 10399–10410, April 11, 2014

Stepwise Organization of the β-Structure Identifies Key Regions Essential for the Propagation and Cytotoxicity of Insulin Amyloid Fibrils*

Received for publication, September 25, 2013, and in revised form, February 4, 2014 Published, JBC Papers in Press, February 28, 2014, DOI 10.1074/jbc.M113.520874

Eri Chatani[‡1], **Hiroshi Imamura**[§], **Naoki Yamamoto**[§], **and Minoru Kato**[§2]

From the [‡]*Department of Chemistry, Graduate School of Science, Kobe University, Hyogo 657-8501, Japan and the* [§]*College of Pharmaceutical Sciences, Ritsumeikan University, Shiga 525-8577, Japan*

Background: Oligomers and protofibrils have been observed in the early stages of fibrillation.
Results: Fibrillation of insulin at a high salt concentration identified a new species of prefibrillar intermediate.
Conclusion: Structural comparison of the intermediate and mature fibrils suggested regions responsible for self-propagation and cytotoxicity.
Significance: The trapping of intermediate is an effective way of revealing molecular details of the organization of fibril structure.

Amyloid fibrils are supramolecular assemblies, the deposition of which is associated with many serious diseases including Alzheimer, prion, and Huntington diseases. Several smaller aggregates such as oligomers and protofibrils have been proposed to play a role in early stages of the fibrillation process; however, little is known about how these species contribute to the formation of mature amyloid fibrils with a rigid cross-β structure. Here, we identified a new pathway for the formation of insulin amyloid fibrils at a high concentration of salt in which mature fibrils were formed in a stepwise manner via a prefibrillar intermediate: minute prefibrillar species initially accumulated, followed by the subsequent formation of thicker amyloid fibrils. Fourier transform infrared spectra suggested the sequential formation of two types of β-sheets with different strength hydrogen bonds, one of which was developed concomitantly with the mutual assembly of the prefibrillar intermediate to form mature fibrils. Interestingly, fibril propagation and cellular toxicity appeared only after the later step of structural organization, and a comparison of β-sheet regions between the prefibrillar intermediate and mature fibrils using proteolysis led to the proposal of specific regions essential for manifestation of these properties.

Amyloid fibrils are β-sheet-rich protein assemblies that are often associated with more than 30 serious amyloidoses (1–3). Moreover, various proteins and peptides not related to amyloidosis have been shown to form amyloids or amyloid-like aggregates, which suggests the potential of amyloid fibrils as a common and unique form of polypeptides as well as native structures (4). Amyloid fibrils are generally formed through nucleation and growth phases. On the basis of this fundamental scheme, nucleation is one of the most important events controlling the pathogenesis and propagation of diseases: many previous reports have shown that nucleation progresses at an extremely low rate, whereas the growth phase proceeds promptly via the incorporation of monomers or oligomers into the ends of nuclei according to a mechanism of template-dependent propagation of the amyloidogenic conformation once nuclei are formed (2, 5). Furthermore, recent experimental studies have proposed the cytotoxic nature of oligomers; therefore, the role of prefibrillar intermediates in diseases has also been a focus (6–11). Given these findings, elucidating the mechanisms for the formation of amyloidogenic nuclei in detail is essential for clarifying the pathogenesis and propagation of amyloidoses at the molecular level. Nevertheless, much remains unknown regarding how and when precursor protein molecules assemble to convert themselves into the amyloidogenic conformations responsible for manifestation of cytotoxicity and propagation behaviors. Although the native protein folding process has been extensively studied, the process of fibrillation needs to be clarified in more detail to understand the exact mechanisms of cross-β assembly.

To address this issue, it is very beneficial to trap and characterize prefibrillar intermediates, which will provide valuable insights into the detailed mechanisms by which the cross-β structure is organized during nucleation as well as the role of oligomers in diseases. The presence of smaller aggregates such as oligomers and protofibrils formed during the nucleation process has recently been revealed experimentally for several proteins. Various techniques such as solid-state NMR (7), small angle x-ray scattering (12, 13), site-directed labeling of fluorescence probes (8), hydrogen/deuterium (H/D) exchange experiments (14), and immunological assays (6) have revealed the structural details of the prefibrillar oligomers involved in fibrillation. However, quantifying and characterizing their physico-

* This work was supported by Ministry of Education, Culture, Sports, Science, and Technology in Japan KAKENHI Grant 23770188, and grants from the Astellas Foundation for Research into Metabolic Disorders, Hayashi Memorial Foundation for Female Natural Scientists, and Tomizawa Foundation (to E. C.), and the Ritsumeikan Global Innovation Research Organization (R-GIRO) (to M. K.).

[1] To whom correspondence may be addressed: 1-1 Rokkodai, Kobe, Hyogo 657-8501, Japan. Tel.: 81-78-803-5673; Fax: 81-78-803-5673; E-mail: chatani@crystal.kobe-u.ac.jp.

[2] To whom correspondence may be addressed: 1-1-1 Noji-Higashi, Kusatsu, Shiga 525-8577, Japan. Tel.: 81-77-561-2761; Fax: 81-77-561-2659; E-mail: kato-m@ph.ritsumei.ac.jp.

chemical properties are often hampered due to their unstable and heterogeneous properties; therefore, it is very difficult to clarify how these species contribute to the formation of mature fibrils with a rigid β-sheet core.

Here, we investigated a fibrillation pathway of insulin in which oligomer- or protofibril-like prefibrillar intermediate species could be detected in the early stages of fibrillation. Insulin is a hormone protein associated with glucose metabolism and consists of two polypeptide chains (*i.e.* A-chain of 21 amino acid residues and B-chain of 30 amino acid residues) connected by two intermolecular disulfide bonds. Insulin is one of the most important subjects in the field of diabetes therapy, and it has also become one of the best models for investigating fibrillation mechanisms in the past few decades by readily forming amyloid fibrils *in vitro* (15). By incubating insulin at a high temperature and in the presence of a high concentration of salt, we identified a new pathway for the formation of insulin amyloid fibrils in which a large amount of immature intermediate fibrils accumulated prior to the formation of mature fibrils. The sequential formation of β-sheet structures with different strength hydrogen bonds was clarified in this pathway, and in conjunction with this stepwise β-sheet organization, self-propagating ability, and cellular cytotoxicity manifested only at a later stage of the process. By comparing β-sheet regions in prefibrillar intermediates with those in mature fibrils using proteolytic analysis combined with mass spectrometry, we identified the amino acid regions responsible for propagating ability and cytotoxicity, based on which the detailed molecular mechanisms of fibril formation have been discussed.

EXPERIMENTAL PROCEDURES

Heat-induced Fibril Formation—The spontaneous formation of insulin amyloid fibrils without seeds was performed by heating. A total of 1.0 mg/ml of bovine insulin (Sigma) was dissolved in 25 mM HCl (pH 1.6) containing 0, 0.1, or 1.0 M NaCl. 500-μl aliquots of the sample solutions were transferred to 1.5-ml polypropylene test tubes and heated from room temperature to 90 °C at a rate of ~2 °C/min using a heat block (Dry Thermo Unit DTU-1B; TAITEC, Nagoya, Japan). After reaching 90 °C, the samples were removed from the heat block and air-cooled back to room temperature with gentle mixing; the temperature dropped to below 30 °C within 5 min. After 20 min, a 7.5-μl aliquot of the sample was mixed with 1.5 ml of 5 μM thioflavin T (ThT)[3] in 50 mM glycine-NaOH buffer (pH 8.5) at 25 °C, and the fluorescence intensity at 485 nm of this solution was measured with an excitation wavelength of 445 nm to assay the formation of amyloid fibrils (16). Samples were then heated again, a process that was repeated three times. The fibrillation time course was also examined by measuring ThT fluorescence at different time points immediately after increasing the temperature to various levels from 55 to 90 °C to initiate the fibrillation reaction. For this experiment, 500-μl aliquots of the sample solutions sealed in the 1.5-ml polypropylene test tubes were immersed in the heat block, which had been preheated to the reaction temperature; under this condition, the temperature jump of sample solutions was completed within 5 min. Insulin concentrations were determined using an absorption coefficient of 1.0 for 1.0 mg/ml at 276 nm (17).

Atomic Force Microscopy (AFM)—A total of 10 μl of fibril samples was spotted onto a freshly cleaved mica plate. The residual solution was removed after 1 min by placing a piece of filter paper at the edge of the mica plate followed by drying. AFM images were obtained using a Nano Scope IIIa (Digital Instruments, Tonawanda, NY). The scanning tip used was a phosphorus (*n*)-doped Si (Veeco Instruments, Plainview, NY; spring constant = 20–80 N/m, resonance frequency = 245–289 kHz), and the scan rate was 0.5 Hz.

Fourier Transform Infrared (FTIR) Absorption Measurement—FTIR spectra were measured with a FT/IR-6100 model spectrometer equipped with a DLATGS detector (Jasco, Tokyo, Japan) and a water-circulating system connected to a thermoregulated water bath. Samples for the structural analysis of heat-induced fibrils were precipitated by centrifugation to concentrate the fibrils to ~10 mg/ml, and washed with a small amount of D_2O solution containing 25 mM DCl and 0.1–1.0 M NaCl three times prior to the measurement to diminish the amount of contaminated water interfering with the observation of the amide I band region. Samples were sealed with a cell with CaF_2 windows and a 50-μm polytetrafluoroethylene spacer, and the FTIR spectrum was monitored at room temperature by collecting 256 interferograms with a resolution of 2 cm^{-1}. To time course monitor fibril formation, 10 mg/ml of native insulin solution dissolved in 25 mM DCl containing 1.0 M NaCl was used as a sample. Prior to the sample preparation, native insulin was preincubated in 25 mM DCl and at 37 °C for 24 h to complete the H/D exchange of amide protons. Samples were then sealed with the 50-μm optical path-length CaF_2 cell embedded inside the water-circulating system, and the temperature of the sample liquid was immediately raised to the measurement temperature (*i.e.* 75 or 90 °C) within several minutes to initiate the fibrillation reaction. The first FTIR spectrum was monitored 5 min after the temperature increase and subsequent spectra were collected at an interval of 4 min at a constant temperature.

Seed-dependent Fibril Extension—The seed-dependent extension reaction was examined by adding sonicated fibrils as seeds to native insulin in a 25 mM HCl solution containing 100 mM NaCl at concentrations of 30 μg/ml and 0.3 mg/ml, respectively. To prepare seeds, fibrils were sonicated using a Microson sonicator (Misonix, Farmingdale, NY) at an intensity level of 2 and 20 1-s pulses. The extension reaction was carried out at 37 °C without agitation and the reaction was monitored at different time points by ThT fluorescence analysis.

Cytotoxic Assay—Pheochromocytoma (PC12) cells were grown in Dulbecco's modified Eagle's medium (DMEM) supplemented with 10% heat-inactivated horse serum and 5% fetal bovine serum. PC12 cells were plated on poly-L-lysine-coated dishes for differentiation, and cultured in DMEM supplemented with 10 ng/ml of nerve growth factor. Aliquots of the prefibrillar intermediate or mature fibrils were then added to cell cultures at a final concentration of 8.5 μM, and cells were incubated in a humidified 5% CO_2 at 37 °C for 48 h. Prior to the assay, fibril samples were subjected to 20 pulses of sonication using a Microson sonicator at an intensity level of 2 to improve

[3] The abbreviations used are: ThT, thioflavin T; AFM, atomic force microscopy; FTIR, Fourier transform infrared; H/D, hydrogen/deuterium.

dispersion by breaking up fibril clumps. Cell death was evaluated by measuring the extent of release of lactate dehydrogenase intracellularly to the medium using a commercial CytoTox 96 Non-radioactive Cytotoxicity Assay (Promega, Madison, WI). All measurements were performed three times and the percentage of surviving cells was calculated by assuming the value obtained by the addition of solvent only (*i.e.* HCl and NaCl at final concentrations of 1.25 and 50 mM, respectively) to be 100%. Statistical analysis was performed by one-way factorial analysis of variance combined with Scheffe's test for all paired comparisons, where $p < 0.05$ was considered statistically significant.

Proteolytic Digestion of Prefibrillar Intermediate and Mature Amyloid Fibrils—Intermediate and mature fibrils were prepared by incubating 5 mg/ml of insulin solution dissolved in 25 mM HCl containing 1.0 M NaCl at 75 °C for 1 and 3 h, respectively. The enzymatic digestion of these fibrils was performed by mixing 200 μl of 0.63 mg/ml of pepsin from porcine gastric mucosa with 500 μl of the sample solution and incubating at 37 °C for 24 h. After the proteolytic treatment, samples were centrifuged and the pellet was washed 3 times with 25 mM HCl containing 1.0 M NaCl. The pellet was then solubilized by suspending it in dimethyl sulfoxide and incubating at 25 °C for over 10 h. The reduction of disulfide bonds was performed by adding 50 times its volume of 20 mM Tris-HCl buffer (pH 7.0) containing 10 mM dithiothreitol (DTT), followed by incubation at 50 °C for 1 h. The free cysteine residues generated were carboxyamidomethylated by adding 5 times its volume of 100 mM iodoacetamide dissolved in 100 mM Tris-HCl (pH 7.0), which was incubated by agitating at 25 °C for 40 min. Measuring the matrix-assisted laser desorption ionization-time-of-flight (MALDI-TOF) mass spectra of the obtained peptide fragments was performed with a Voyager DE-STR MALDI-TOF mass spectrometer (Applied Biosystems) using α-cyano-4-hydroxycianamic acid as a matrix.

RESULTS

Formation of Prefibrillar Intermediate Fibrils in the Presence of a High Concentration of NaCl—We first investigated the effects of the concentration of NaCl on the formation of insulin amyloid fibrils, which was monitored with the ThT binding assay (Fig. 1, *A–C*). Earlier studies revealed the spontaneous formation of insulin amyloid fibrils when subjected to high temperatures under acidic conditions (18–20). In the present study, bovine insulin dissolved in 25 mM HCl was commonly used as a fundamental solution and three different concentrations of NaCl, *i.e.* 0, 0.1, and 1.0 M, were analyzed. Regarding the heating method, we employed a linear heat gradient from 25 to 90 °C, which was convenient for rapidly assessing fibrillation.

When insulin was heated in the absence of NaCl, no increase in ThT fluorescence was observed in the sample solution, even after three cycles of heat treatment (Fig. 1*A*). In contrast, a significant increase in ThT fluorescence was observed after the 1st cycle of heating in the presence of 0.1 M NaCl, the salt condition most frequently used for insulin fibrillation, which indicated the formation of amyloid fibrils consistent with previous reports on the NaCl-induced enhancement of insulin fibril formation (Fig. 1*B*) (17, 21). Fibrillation was completed within the

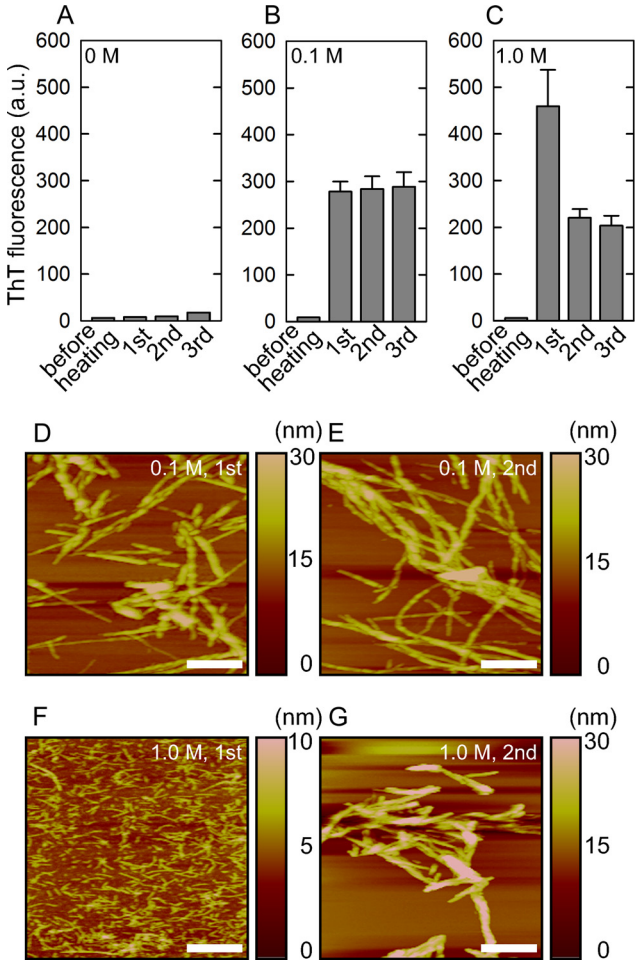

FIGURE 1. **Effects of salt concentration on the heat-induced spontaneous fibrillation reaction of insulin amyloid fibrils.** *A–C*, ThT fluorescence intensity measured before and after the 1st, 2nd, and 3rd cycles of the periodic heat treatment with a linear gradient of temperature from 25 to 90 °C at a rate of 2 °C/min. The results of NaCl concentrations of 0 M (*A*), 0.1 M (*B*), and 1.0 M (*C*) are shown. All measurements were performed three times and the *error bars* depict the S.D. ± mean. *D–G*, AFM images of insulin fibrils formed by heat-induced fibrillation. The amyloid fibrils formed at 0.1 and 1.0 M NaCl were sampled after the 1st and 2nd cycles of heat treatment in the presence of 0.1 M (*D*, 1st; *E*, 2nd) and 1.0 M (*F*, 1st; *G*, 2nd) NaCl. The *scale bars* represent 500 nm.

1st cycle of heating and almost the same ThT fluorescence intensity was maintained after the 2nd and 3rd cycles of the heating treatment. AFM images verified the formation of typical amyloid fibrils with needle-like morphology, and fibril height or length appeared to be unchanged after the 2nd heating cycle, which was in accordance with the unaltered ThT fluorescence intensity (Fig. 1, *D* and *E*).

Interestingly, when insulin was heated in the presence 1.0 M NaCl, the intensity of ThT fluorescence was markedly higher than that observed at 0.1 M NaCl, and the intensity was subsequently decreased by half after the 2nd heating cycle (Fig. 1*C*). This two-step change in fluorescence intensity implied the transient accumulation of different conformations with distinct ThT binding properties from that of mature fibrils, considering that the intensity of ThT fluorescence is determined by the affinity of ThT-binding sites, number of ThT-binding sites, and ThT fluorescence strength for each bound state as well as the amount of fibrils. To test this possibility, the sample was subjected to AFM analysis. In line with our expectations, AFM

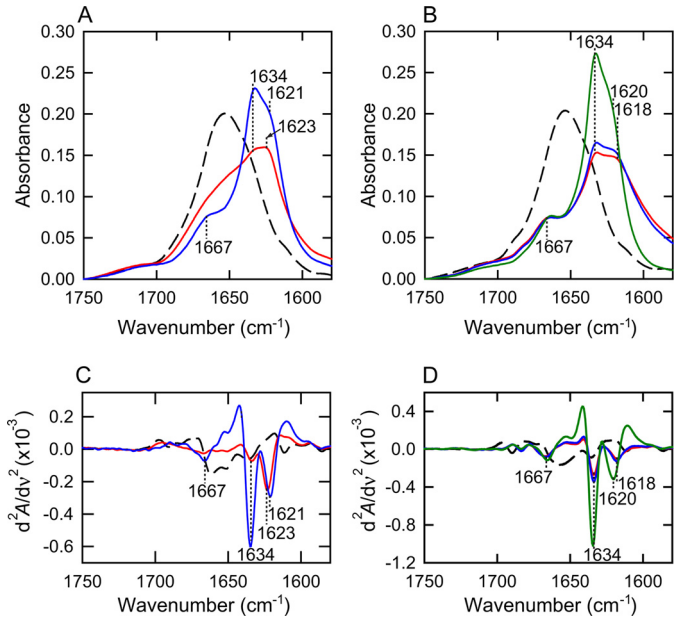

FIGURE 2. **FTIR absorption spectra of insulin amyloid fibrils obtained by repeated cycles of the heat treatment.** *A* and *B*, the spectra at approximately the amide I region of fibrils formed after the 1st (*red*) and 2nd (*blue*) cycles of heat treatment at 1.0 M (*A*) and 0.1 M NaCl (*B*). FTIR measurements were performed at 25 °C. The *black dashed lines* represent the spectra of native insulin without any heat treatment as a reference. The spectrum of amyloid fibrils formed by repeated self-seeding at 0.1 M NaCl was also shown in a *green line* for reference. Spectra were normalized so that the integrated intensity of the amide I band ranging from 1580 to 1750 cm^{-1} was set to be equal. *C and D*, second-derivative infrared spectra at 1.0 M (*C*) and 0.1 M NaCl (*D*). The colors are the same as those in *panels A* and *B*.

images exhibited the dominance of very thin and short aggregates (Fig. 1*F*), which suggested the transient accumulation of a prefibrillar intermediate. Needle-like morphology appeared after the 2nd heat treatment (Fig. 1*G*). The average height values obtained by sampling 10 different fibrils were 2.5 ± 0.4 nm for the prefibrillar intermediate and 10.4 ± 3.1 nm for the mature fibrils. Therefore, we postulated that the second step accompanying the reduction in ThT fluorescence intensity was attributed to the maturation process toward longer and thicker amyloid fibrils.

When FTIR spectroscopy was performed to compare microscopic structures between the intermediate-like species and mature fibrils formed after the 1st and 2nd cycles of heating at 1.0 M NaCl, respectively, the obtained spectra revealed a marked difference in shape in the amide I region (Fig. 2). The amyloid fibrils of bovine insulin were previously shown to exhibit two peaks associated with β-sheet structures at two different frequencies (22, 23). In accordance with previous findings, the mature fibrils exhibited a sharp main peak at 1634 cm^{-1} with a shoulder at 1621 cm^{-1}, in addition to a shoulder at ~1667 cm^{-1}, which revealed the intermolecular β-sheet-rich structure with a small amount of turns and/or loops. However, intermediate fibrils showed a markedly broader shape than that of mature fibrils, although the main band at 1623 cm^{-1} suggested the partial formation of a β-sheet structure (Fig. 2*A*). Second derivative spectra were also produced to emphasize the positions of these peaks, as shown in Fig. 2*C*. The derivative spectrum of mature fibrils formed in the present study showed two sharp minimum peaks at 1621 and 1634 cm^{-1}. On the other hand, intermediate fibrils showed only one peak at 1623 cm^{-1} that was noticeable, whereas that at 1634 cm^{-1} was almost absent, supporting the incomplete organization of β-sheet structure characteristic to the prefibrillar intermediate. The amyloid fibrils formed at 0.1 M NaCl exhibited two sharp minimum peaks at 1618 and 1634 cm^{-1} both after the 1st and 2nd cycles of heating (Fig. 2, *B* and *D*), in agreement with the unchanged fibril structures indicated by AFM and ThT fluorescence intensity.

To investigate whether the FTIR peaks at 1621 and 1634 cm^{-1} are assigned to cross-β structures, x-ray diffraction was analyzed supplementarily for the prefibrillar intermediate and mature fibrils. The diffraction patterns clearly supported the presence of cross-β structure both for the intermediate and mature fibrils by exhibiting two intense reflections at ~4.8 and ~11 Å, although the poor quantitativity of powder diffraction data hampered to verify an increased amount of the cross-β structure for the mature fibrils compared with that for the prefibrillar intermediate species (data not shown). Consequently, at least the FTIR intermolecular β-sheet band at 1621 cm^{-1} was assigned to the cross-β structure, failing to the exact assignment of the peak at 1634 cm^{-1}.

Time Course for the Accumulation of an Intermediate Structure—To further explore the kinetic features for the formation of intermediate fibrils, the time course of fibril formation at 1.0 M NaCl was monitored by ThT fluorescence at varying temperatures ranging from 55 to 90 °C. A marked increase in ThT fluorescence was promptly observed after initiating the reaction at 75 °C and above, which then gradually decreased, representing the transient accumulation of intermediate fibrils (Fig. 3*A*). The two-phase change in ThT fluorescence specifically appeared to be observed at high temperatures only: the population of intermediate fibrils with high ThT fluorescence intensity in the range of 60 to 70 °C was not as large as that observed at higher temperatures, and the pattern appeared to migrate toward a typical sigmoidal pattern with a lag phase followed by extension as the incubation temperature became lower (Fig. 3*B*). No increase in ThT fluorescence intensity was observed within the experimental period at 55 °C (Fig. 3*B*). When spontaneous fibril formation was monitored at 0.1 M NaCl, the time course showed a typical sigmoidal pattern even at 90 °C, without the accumulation of prefibrillar intermediate species with high ThT fluorescence intensity (Fig. 3*C*).

We further investigated the β-sheet structure organization using real-time monitoring of FTIR spectroscopy forming insulin fibrils inside an optical cell (Fig. 4). Amide I absorption bands shifted slightly toward shorter wavenumbers to be represented as amide I′ because all of the amide protons of the insulin sample were substituted by deuterium prior to initiation of the fibrillation reaction for this measurement (see "Experimental Procedures"). When monitored at 75 °C, development of the β-sheet peak at 1619 cm^{-1} was observed immediately after elevating the temperature, which confirmed the abrupt formation of prefibrillar intermediate fibrils with a partial amount of β-sheet structures (Fig. 4, *A*, *C*, and *E*). However, the subsequent development of another β-sheet peak at 1628 cm^{-1} was significantly delayed, failing to be observed within the present experimental time period. The retardation of this later mat-

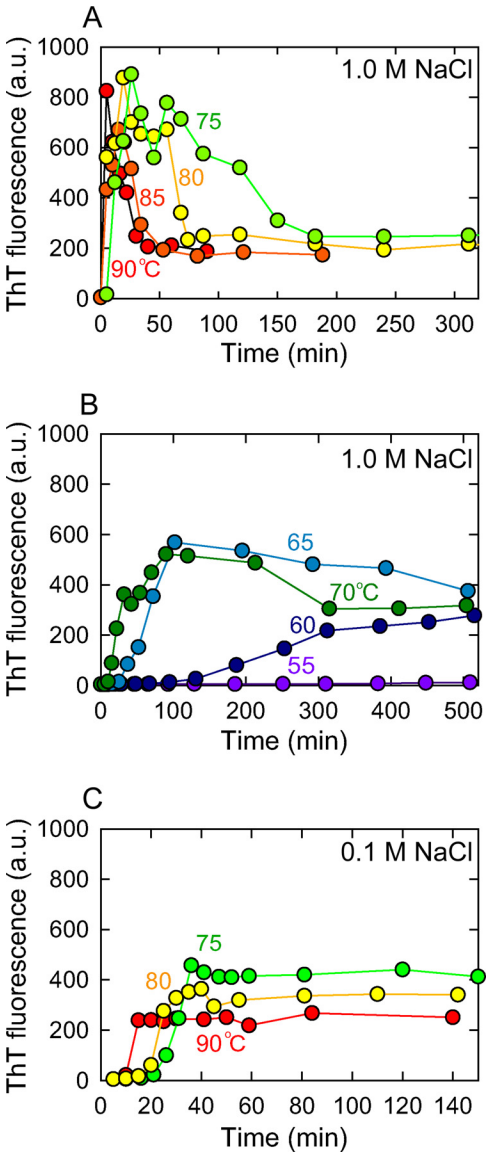

FIGURE 3. **Dependence of temperature and salt concentration on the transient accumulation of prefibrillar intermediates.** The time course for the spontaneous formation of insulin amyloid fibrils in the presence of 1.0 (*A* and *B*) or 0.1 M NaCl (*C*) at different temperatures was monitored using ThT fluorescence. *A*, the time course for the formation of insulin amyloid fibrils in the presence of 1.0 M NaCl at 90 (*red*), 85 (*orange*), 80 (*yellow*), and 75 °C (light green), and *B*, 70 (*green*), 65 (*cyan*), 60 (*dark blue*), and 55 °C (*purple*). *C*, the time course in the presence of 0.1 M NaCl at 90 (*red*), 80 (*yellow*), and 75 °C (*light green*), in which no abrupt increase in ThT fluorescence intensity was observed immediately after the temperature increase.

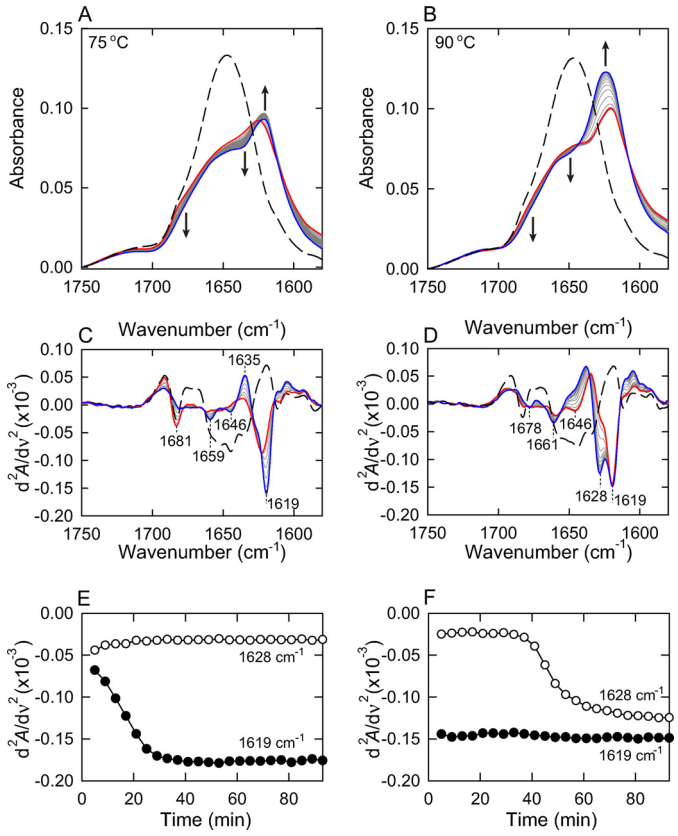

FIGURE 4. **FTIR real-time monitoring of the organization of the cross-β structure.** Time-dependent changes in the FTIR absorption spectra were monitored in the presence of 1.0 M NaCl at two different high temperatures. *A* and *B*, FTIR absorption spectra during the fibrillation reaction at 75 (*A*) and 90 °C (*B*). In both panels, the 1st spectrum was monitored 5 min after initiation of the reaction and the last spectrum are represented by *red* and *blue lines*, respectively, and the spectra at intervals of 4 min during the first and last traces are represented by *gray lines*, as guided by *arrows*. The spectra of insulin before the heat treatment are also shown by *black dashed lines*. *C* and *D*, second-derivative infrared spectra at 75 (*C*) and 90 °C (*D*) are also shown. The *line colors* are the same as those in *panels A* and *B*. *E* and *F*, time-dependent changes in the values of second-derivative infrared spectra monitored at 1619 cm^{-1} (●) and 1628 cm^{-1} (○).

uration process may have been due to adsorption of the prefibrillar intermediate on the surface of CaF_2 windows with which the sample liquid contacts in a large area due to the very short path length (50 μm). When the reaction speed was accelerated by raising the temperature to 90 °C, the appearance of the peak of the β-sheet structure at 1628 cm^{-1} was successfully observed, although the β-sheet structure at 1619 cm^{-1} already formed within a dead time before the first scan of the FTIR spectrum (Fig. 4, *B*, *D*, and *F*). Overall, the combination of experiments with two different temperatures revealed the sequential formation of these two types of β-sheets with different strength hydrogen bonds: as was seen in the time-dependent changes in the values of secondary derivatives at 1619 and 1628 cm^{-1}, a β-structure with stronger hydrogen bonds was initially organized to form protofibril-like intermediates with thin and short morphology as a first step, and these intermediate fibrils were further mutually assembled to form mature fibrils with needle-like morphology in the later maturation process by forming another type of β-structure with weaker hydrogen bonds (Fig. 4, *E* and *F*). Although competitive amplification of a subpopulation of a different type of fibrils, bearing no relationship to the maturation process, should also be considered as an alternative possibility to explain the appearance of the β-sheet peak at 1628 cm^{-1}, a similar shape of the time dependence in the values of the second derivative infrared spectra monitored at 1628 cm^{-1} during the maturation process (Fig. 4*F*, *open circles*) with that in ThT fluorescence intensity (Fig. 3*A*) suggests strong coupling of the change in the FTIR peak at 1628 cm^{-1} to the maturation process. Furthermore, FTIR spectrum of insulin fibrils measured after the repetitive self-seeding reactions showed conservation of the two different β-sheet peaks in the similar proportion (Fig. 2, *B* and *D*); if two types of fibrils coexisted independently, the population of one

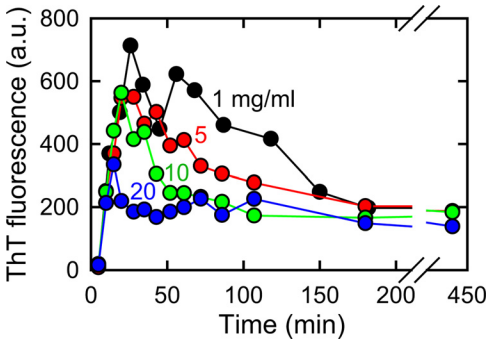

FIGURE 5. **Effect of protein concentrations on accumulation of the prefibrillar intermediate of insulin amyloid fibrils.** Time course for the spontaneous formation of insulin amyloid fibrils in the presence of 1.0 M NaCl was monitored at 75 °C using ThT fluorescence at different concentrations of protein, *i.e.* 1 (*black*), 5 (*red*), 10 (*green*), and 20 mg/ml (*blue*). ThT fluorescence intensity was divided by protein concentration for plots of measurements at 5, 10, and 20 mg/ml of insulin to bring their level in line with that at 1 mg/ml.

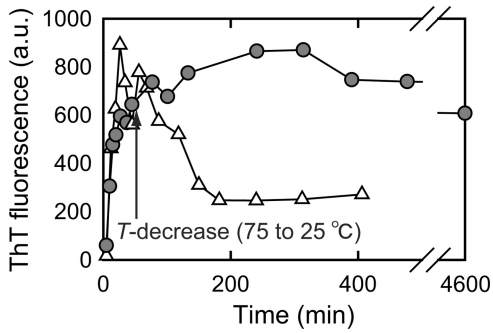

FIGURE 6. **Trapping of the prefibrillar intermediate of insulin by cooling to room temperature.** Intermediate fibrils were formed by incubating insulin at a concentration of 1 mg/ml dissolved in 25 mM HCl containing 1.0 M NaCl at 75 °C, and after accumulation of the prefibrillar intermediate, which was indicated by a markedly higher ThT fluorescence intensity, the reaction temperature was decreased to 25 °C and then the population of prefibrillar intermediate was monitored using ThT fluorescence intensity (*gray circles*). The time point of the temperature decrease is marked by an *arrow*. The result without a temperature decrease (*i.e.* the result of constantly incubating at 75 °C throughout the experiment; Δ) is also represented for comparison.

with a slow growth rate would be diminished as a result of competitive propagation (24). The synchronous propagation of these two FTIR peaks thus also supports the idea that the appearance of peak at 1628 cm^{-1} is assigned to the structural maturation of fibril internals through mutual assembling of intermediate fibrils, rather than the formation of additional exogenous by-products. The maturation process appeared to be accelerated by an increase in the protein concentration, which indicated that the prefibrillar intermediate fibrils may directly contribute to the maturation process by playing the role of an on-pathway intermediate (Fig. 5). Additionally, when the prefibrillar intermediate fibrils were centrifuged at 14,000 rpm (18,700 × *g*) for 1 h at 25 °C and the concentration of residual insulin molecules remaining inside the supernatant was determined using UV absorbance measurement, only a small amount of residual proteins, less than 30 μg/ml, remained after the formation of the prefibrillar intermediate (data not shown), supporting the idea that the prefibrillar intermediate converts directly to mature fibrils.

Relationship between the Organization of the β-Structure, Self-propagation, and Cytotoxicity of Amyloid Fibrils—To investigate the structure-function relationship of amyloid fibrils, we examined the seeding effects and cytotoxicity of prefibrillar intermediate and mature amyloid fibrils. The intermediate species was stable at room temperature and when the reaction temperature decreased to 25 °C after accumulation of the prefibrillar intermediate, the high ThT fluorescence intensity characteristic of the prefibrillar intermediate was maintained at room temperature for more than 72 h, which suggested that prefibrillar intermediate fibrils could survive for a longer time period without any progression in their structural conversion to mature fibrils (Fig. 6); therefore, we used the trapped intermediate fibrils for subsequent investigations.

Self-propagation, which can be assessed by seed-dependent extension reactions in the presence of preformed fibrils as seeds, is considered to be one of the most characteristic features of amyloid fibrils underlying the transmissibility of amyloidogenic diseases (11). The addition of mature amyloid fibrils to a newly prepared insulin solution led to an exponential increase in ThT fluorescence intensity without a lag phase for all fibrils, which showed that mature fibrils strongly influenced self-propagation (Fig. 7*A*). In contrast, the prefibrillar intermediate fibrils did not enforce the self-propagation reaction without any pronounced elongation for several hours, which suggested that the intermediate species did not serve as nuclei for fibril formation. Although a longer incubation led to a gradual increase in ThT fluorescence intensity to a similar value as that of mature fibrils, this reaction was presumably caused by an indirect role of the intermediate fibrils on secondary nucleation enhanced onto a hydrophobic surface of the intermediate, or alternatively by a seeding effect to form prefibrillar intermediates from native insulin molecules (25).

We also analyzed the cytotoxicities of intermediate and mature fibrils using cell viability assays with PC12, a rat adrenal pheochromocytoma cell line. An increasing number of studies have suggested that early stage aggregates in the fibril formation process are more toxic than mature fibrils (6–10). Although the severe toxic nature of prefibrillar intermediates was initially expected based on the findings of these reports, cytotoxicity was observed only for the mature fibrils and the intermediate species was nearly non-toxic to a similar level as that of non-aggregated intact insulin (Fig. 7*B*). Slight excess over 100% observed for the intact insulin and prefibrillar intermediate can be attributed to insulin-enhanced division of neuronal cells. Although the result for the cellular toxicity of the intermediate fibrils was contrary to what was expected, it is clear that structural differences between the intermediate and mature amyloid fibrils led to their distinctive toxicity and self-propagation properties. Based on the two-step change in the FTIR spectrum in the amide I′ region, the β-sheet structure formed in the second maturation step was confirmed to be the key region responsible manifesting the self-propagation and cytotoxicity of insulin amyloid fibrils.

Identification of the β-Sheet Regions Responsible for Propagation and Cytotoxicity—We performed a limited proteolysis experiment to specify the β-sheet region(s) organized during the maturation process. Proteolysis is one of the most promising methods that can be used to elucidate the β-sheet core regions of amyloid fibrils, and several studies have demonstrated that the flexible regions of amyloid fibrils were suscep-

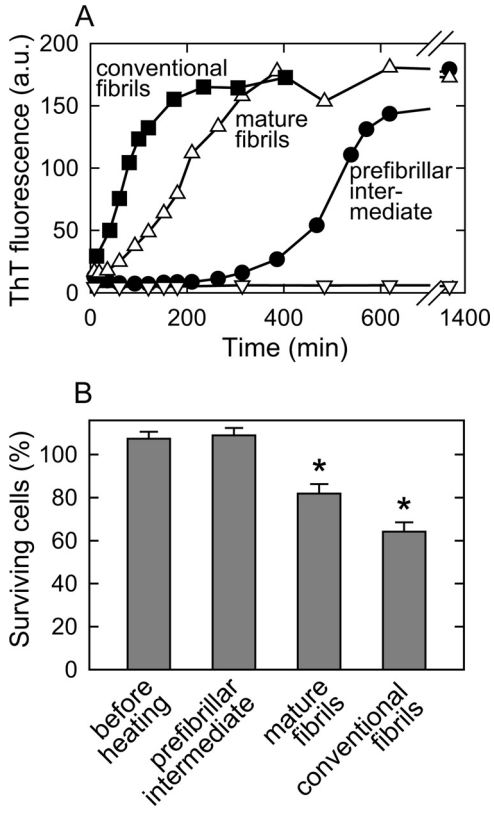

FIGURE 7. **Self-seeding effect and cytotoxicity of prefibrillar and mature amyloid fibrils.** The prefibrillar intermediate and mature fibrils formed by heat treatment in the presence of 1.0 M NaCl were used as seeds. *A*, the time course for the seed-dependent extension reactions performed in a 25 mM HCl solution containing 0.1 M NaCl. In these reactions, 30 μg/ml of prefibrillar intermediate (●) and mature fibrils (Δ) were seeded. The time courses in the absence of seeds (*open inverted triangles*) and presence of conventional insulin fibrils obtained by repeated self-seeding at 0.1 M NaCl (■) were also plotted for negative and positive controls, respectively. *B*, cytotoxic effect in PC12 cells upon the addition of native insulin without heat treatment for prefibrillar intermediate, mature fibrils, and conventional insulin fibrils obtained by the repeated self-seeding of fibrils originally formed at 0.1 M NaCl. The concentration of fibrils added was 8.5 μM and the incubation time was 48 h. Fractions of surviving cells, which were calculated from the activity of lactate dehydrogenase released from dead cells, are represented in this figure. All measurements were performed three times and the *error bars* depict the S.D. ± mean. *, $p < 0.0001$.

tible to digestion by proteases, whereas the core regions were resistant (26–28). In this study, intermediate and mature fibrils were digested by pepsin for 24 h and the fragments produced were analyzed by MALDI-TOF mass spectrometry. We estimated that the regions susceptible to proteolytic cleavage only for the prefibrillar intermediate would correspond to the β-sheet region(s) organized during the later maturation process, *i.e.* the region(s) important for the self-propagation and cellular toxicity of insulin amyloid fibrils.

As a result of the proteolytic treatment, both mature fibrils and the prefibrillar intermediate appeared to be resistant to proteolysis as FTIR spectra revealed that their secondary structures were almost intact even after the 24-h digestion (data not shown). This was in contrast to the rapid digestion of native insulin by pepsin (29), and under the present conditions, native insulin was cleaved into fragments smaller than 1,500 Da after an incubation period of only 2 h (data not shown). However, when samples were dissolved by dimethyl sulfoxide and disulfide bonds were then reduced and carboxyamidomethylated, which helped as an indicator for cysteine residues in the mass assignment of peptide fragments, a significant number of peaks derived from peptide fragments were detected by mass spectra, which showed that proteolytic cleavage progressed inside the prefibrillar intermediate and mature fibril samples (Fig. 8*A*). The number of peaks of intermediate fibrils was clearly larger than that of mature fibrils, supporting the immature property of the intermediate fibril structure with a larger amount of flexible regions.

On the basis of the m/z values observed, almost all of the peptide fragments were successfully identified, as summarized in Table 1. Additionally, because the efficiency of ionization in mass spectrometry was shown to be markedly lower for the isolated A-chain peptide or its derivative fragments than for the B-chain peptide (30), the mass spectra of samples without reduced disulfide bonds were measured and compared with those of disulfide-reduced and carboxyamidomethylated samples to make up for the identification of digestion sites inside the A-chain. By performing this measurement, several peaks derived from A-peptide fragments, each of which was connected to a B-peptide fragment with an intermolecular disulfide bond, were observed for the intermediated fibrils, from which two additional cleavage sites on the A-peptide were identified (Fig. 8*B* and Table 2). No cleavage site was found inside the A-peptide for the mature fibrils. Three regions susceptible to proteolysis only for the prefibrillar intermediate fibrils, *i.e.* A:13–16, B:4–5, and B:11–17, have been proposed as candidates for the key regions responsible for the propagation and cytotoxicity of insulin amyloid fibrils (Fig. 8*C*, *green regions*).

DISCUSSION

A New Species of Prefibrillar Intermediate Detected by Salt-induced Perturbation of the Fibrillation Pathway—The transient formation of several oligomer- or protofibril-like immature species have so far been reported for the fibrillation of insulin (12, 23, 31–35). Their population and properties appeared to be highly dependent upon the reaction conditions such as the concentrations of proteins, solvent composition, and incubating temperature or pressure, which suggested that the phase boundary between monomers and prefibrillar intermediates was sensitively perturbed by these external factors. In agreement with these results, a theoretical study recently proposed that even a slight perturbation in solution conditions can drive the fibrillation pathway toward the system in which oligomers are present as a stable intermediate phase (36). Here, we identified a new pathway for the formation of insulin amyloid fibrils by combining a high concentration of NaCl and high temperature, in which characteristic prefibrillar intermediate fibrils accumulated prior to the formation of mature fibrils. One of the most characteristic properties of this intermediate species is its markedly higher ThT fluorescence intensity, which might have resulted from a larger surface area of the prefibrillar intermediate per weight concentration compared with that of mature fibrils and then served as a clear sign of the presence of intermediate species with an unconventional time-dependent pattern (Figs. 1*C* and 3*A*); however, the exact reasons why ThT fluorescence intensity for the prefibrillar intermediate with an

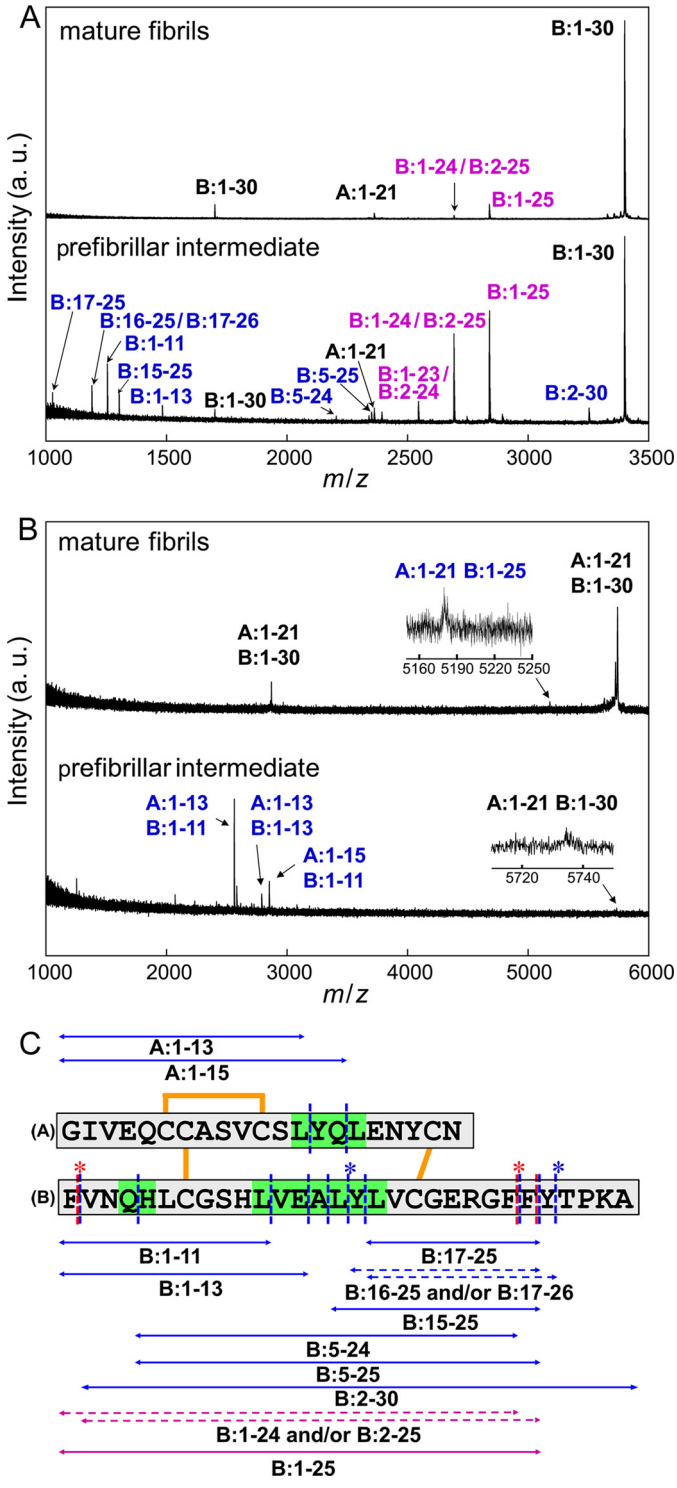

FIGURE 8. **Identification of amino acid regions responsible for manifesting the propagation ability and cytotoxicity.** *A* and *B*, MALDI-TOF mass spectra of peptide fragments of prefibrillar intermediate and mature fibrils. In this study, peptides were identified under two conditions: with (*A*) and without (*B*) the reduction of disulfide bonds inside the insulin molecule. The spectra of mature fibrils and prefibrillar intermediate species are shown on the *upper* and *lower sides* of each panel, respectively, and *blue* and *magenta* labels on the assigned peaks represent peptide fragments found only in the prefibrillar intermediate and in both the prefibrillar intermediate and mature fibrils, respectively. *Black labels* represent peaks derived from an uncleavaged fraction of insulin molecules. Also see Tables 1 and 2 for numerical data on the peaks detected. *C*, summary of the limited proteolysis of the intermediate and mature fibrils insulin by pepsin. The peptides identified by MALDI-TOF mass spectrometry are shown by *double-headed arrows* alongside the primary sequences of the A-chain and B-chain. The *blue* and *magenta arrows* represent peptide fragments found only in intermediate fibrils and those found in both intermediate and mature fibrils, respectively. Cleavage sites are summarized on the primary sequence of insulin, in which *blue* and *red dashed lines* represent the sites cleaved in the intermediate and mature fibrils, respectively. Regarding peptide fragments in which two possible identifications were assigned on the basis of the mass values, both of these possibilities were represented by *dashed double-headed arrows with asterisks* at the corresponding cleavage sites on the primary sequence. The regions sensitive to proteolytic digestion only in the intermediate fibrils are colored *green*.

immature structure was higher than that for mature fibrils remain unknown.

The main effect of salts has generally been considered to be a combination of screening of the electric charge of protein molecules through direct interactions between ions and proteins according to the electroselectivity series and solvent interactions perturbing protein hydration and/or bulk water conditions through indirect water-solute interactions according to Hofmeister series (34, 37). Through these effects, salts have been expected to modulate a balance between the electrostatic and hydrophobic interactions critical for fibrillation (37, 38), and tilting its balance toward stronger hydrophobicity by the presence of high concentrations of salts often results in the formation of worm-like or protofibril-like aggregates (39, 40). In light of the conceptual proposal that the presence of lag time is an essential characteristic by which crystal-like amyloid fibrils are distinguished from glass-like amorphous aggregates (38), the elimination of lag time in the present stepwise pathway (Fig. 3*A*) suggests that the prefibrillar intermediate fibrils assume an intermediary property between crystalline and amorphous structures. It is plausible that salt-induced increments in hydrophobic interactions among insulin molecules promoted the rapid accumulation of metastable prefibrillar intermediate fibrils with less organized immature β-structures.

Candidates of Specific Regions Contributing to the Propagation and Cytotoxicity of Amyloid Fibrils—As an advantageous property of the prefibrillar intermediate found in the present study, it was very stable at room temperature (Fig. 6), which allowed its application to a wide range of structural investigations. This stable population of intermediate fibrils has been attributed to a kinetic trap with an elevated energy barrier that separated the subsequent maturating process at room temperature, as was previously observed for the soluble intermediates of Aβ(1–40) that survived for a much longer time by lowering temperatures (41) and for annealing of the β-sheet core structure of mammalian prion fibrils that only proceeded at high temperatures (42). Through detailed comparison of β-sheet regions between the prefibrillar intermediate and mature fibrils as well as their seeding ability and cellular toxicity, particular peptide regions strongly associated with the propagation and cytotoxicity of insulin amyloid fibrils, have been specified successfully (Fig. 8*C*).

The growing ends of seed fibrils are generally considered to behave like a template in the template-dependent self-propagation mechanism of amyloid fibrils, onto which precursor proteins attach and successively change their conformation to replicate the same template structure, referred to as the dock-lock model (43, 44). Previous pre-steady state kinetic studies performed with Trp fluorescence (45) and H/D exchange com-

TABLE 1

Assignment of the digestive fragments of mature and prefibrillar intermediate fibrils

Fibrils were depolymerized into monomers by the addition of dimethyl sulfoxide after the proteolytic treatment, and the disulfide bonds of the sample were reduced and carboxyamidomethylated before the measurement.

Observed *m/z*[a]	Theoretical *m/z*[a]	Assignment
Mature fibrils		
2339.049	2338.981	GIVEQCCASVCSLYQLENYCN (A:1–21)
2360.988	2360.963	GIVEQCCASVCSLYQLENYCN (A:1–21) $[M + Na]^+$
2392.874		Unmatched
2500.268		Unmatched
2691.387	2691.317	FVNQHLCGSHLVEALYLVCGERGF (B:1–24) and/or VNQHLCGSHLVEALYLVCGERGFF (B:2–25)
2838.413	2838.385	FVNQHLCGSHLVEALYLVCGERGFF (B:1–25)
3398.681	3398.681	FVNQHLCGSHLVEALYLVCGERGFFYTPKA (B:1–30)
Prefibrillar intermediate		
1027.491	1027.503	LVCGERGFF (B:17–25)
1190.564	1190.566	YLVCGERGFF (B:16–25) and/or LVCGERGFFY (B:17–26)
1254.607	1254.605	FVNQHLCGSHL (B:1–11)
1303.655	1303.650	LYLVCGERGFF (B:15–25)
1482.738	1482.716	FVNQHLCGSHLVE (B:1–13)
2203.090	2203.079	HLCGSHLVEALYLVCGERGF (B:5–24)
2338.967	2338.981	GIVEQCCASVCSLYQLENYCN (A:1–21)
2350.191	2350.147	HLCGSHLVEALYLVCGERGFF (B:5–25)
2360.997	2360.963	GIVEQCCASVCSLYQLENYCN (A:1–21) $[M + Na]^+$
2392.938		Unmatched
2544.280	2544.249	FVNQHLCGSHLVEALYLVCGERG (B:1–23) and/or VNQHLCGSHLVEALYLVCGERGF (B:2–24)
2691.344	2691.317	FVNQHLCGSHLVEALYLVCGERGF (B:1–24) and/or VNQHLCGSHLVEALYLVCGERGFF (B:2–25)
2745.272		Unmatched
2838.416	2838.385	FVNQHLCGSHLVEALYLVCGERGFF (B:1–25)
2892.322		Unmatched
3251.629	3251.613	VNQHLCGSHLVEALYLVCGERGFFYTPKA (B:2–30)
3398.681	3398.681	FVNQHLCGSHLVEALYLVCGERGFFYTPKA (B:1–30)

[a] Observed and theoretical *m/z* values were represented as monoisotopic masses.

TABLE 2

Assignment of the digestive fragments of mature and prefibrillar intermediate fibrils monitored without the reduction of disulfide bonds

Fibrils were depolymerized into monomers by the addition of dimethyl sulfoxide after proteolytic treatment and then used for measurement.

Observed *m/z*[a]	Theoretical *m/z*[a]	Assignment
Mature fibrils		
5174.1	5174.0	GIVEQCCASVCSLYQLENYCN (A:1–21) plus FVNQHLCGSHLVEALYLVCGERGFF (B:1–25)
Prefibrillar intermediate		
2560.959	2561.140	GIVEQCCASVCSL (A:1–13) plus FVNQHLCGSHL (B:1–11)
2789.168	2789.251	GIVEQCCASVCSL (A:1–13) plus FVNQHLCGSHLVE (B:1–13)
2852.156	2852.262	GIVEQCCASVCSLYQ (A:1–15) plus FVNQHLCGSHL (B:1–11)

[a] For the mature fibrils, observed and theoretical *m/z* values are represented as averaged masses because mass resolution of the observed peak is insufficient for accurate determination of its monoisotopic mass. For the prefibrillar intermediate, observed and theoretical *m/z* values are represented as monoisotopic masses. The *m/z* value for intact insulin (i.e., A:1–21 plus B:1–30) was excluded from the list.

bined with NMR analysis (46), and R_2 relaxation dispersion and transferred cross-saturation NMR experiments (47) have suggested the presence of short amino acid regions involving the formation of a transient monomer-seed complex within precursor proteins. Considering these findings, our present results appear to have identified such specific sequences that play an essential role as a strong candidate for "template" coding a characteristic fibril structure of insulin.

Interestingly, the specified peptide regions corresponded well with positions with high fibrillation propensity to form the cross-β spine core forming rigid intermolecular steric zippers facing two self-complementary sheets, which has been reported by screening for amyloidogenic short peptide segments (48, 49). By identifying such peptide segments, a novel amylome analysis has recently been developed to predict the amyloidogenicity of proteins (50). The deep involvement of the steric zipper structure in the self-propagating ability has been supported by the inhibition of insulin fibrillation by an octapeptide coding amino acid sequence that forms a steric zipper (LVEALYLV) (51) and the effectiveness of the structure-based design of the peptide inhibitors of amyloid fibril formation for favorable affinity with the steric-zipper structure (52). Regarding the structural basis of cytotoxicity, the steric zipper structure is also more likely to intrude into biomembranes, resulting in cellular dysfunction, although the detailed roles of the steric zipper structure have not yet been elucidated. Curiously, the peptide regions specified in this work also correspond approximately to cleavage sites by insulin degrading enzyme (53), suggesting that insulin degrading enzyme suppresses the deposition of insulin *in vivo* by preferentially cleaning up these key regions with strong amyloidogenic features.

Proposed Model for the Organization of β-Sheet Structures and Implication for the Molecular Basis of Fibril Architecture—On the basis of the present results, a schematic model representing the stepwise formation of the β-sheets of amyloid fibrils with different strength hydrogen bonds is illustrated in Fig. 9. Many prefibrillar intermediates and some amounts of β-sheet structures were observed initially in this pathway. The intermediate formed mutually assembled, accompanying the organization of additional β-sheet structures important for fibril functionality (Figs. 8*C* and 9, *green regions*). This scheme assumed the direct involvement of the prefibrillar species focused on in

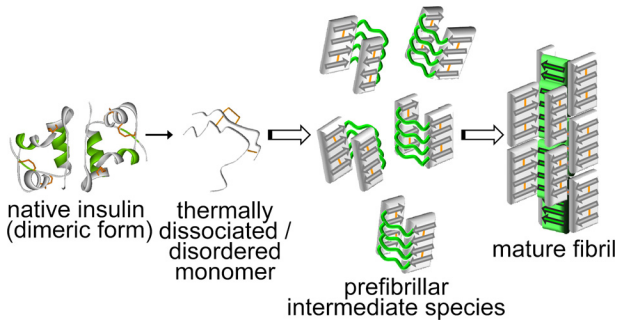

FIGURE 9. **Schematic illustration for the fibril formation of insulin at a high concentration of NaCl.** The regions colored by *green* in the native insulin, prefibrillar intermediate, and mature amyloid fibrils correspond to the regions shown in Fig. 8*C*, and disulfide bonds are represented by *orange lines*. In this illustration, a minimum unit of mature fibrils, *i.e.* protofilament, which further assembles to form a thicker amyloid fibril, is represented as a minimum structure of the mature fibril.

the present study as an on-pathway intermediate playing the role of a conformational unit for the formation of mature amyloid fibrils. When the thickness of the prefibrillar intermediate is postulated to be 2.5 nm on the basis of average height determined from the AFM image, the conjugation of two prefibrillar intermediate fibrils is roughly comparable with the dimensions of a single insulin protofilament (3 × 4 nm) that has been proposed in the previous study of cryo-electron microscopy (54). It is thus plausible that two prefibrillar intermediates assemble mutually to form a protofilament during the maturation process (Fig. 9). Additionally, the average height of mature fibrils (*i.e.* 10.4 nm) suggests that roughly 4 protofilaments further bunch up to form the hierarchical structure of one matured insulin fibril. The organization of two types of β-sheet structures at distinct regions appears to bear a strong resemblance to a recent experimental finding for the fibrillation mechanism of the Sup35NM prion, in which interactions outside the amyloid core drive oligomer formation and subsequently led to the organization of cross-β structures inside the amyloid core region (55).

Whether oligomeric species bear the primary responsibility as an on-pathway intermediate or merely an off-pathway product remains a controversial issue in the mechanisms of amyloid formation (9). Intermediates have been regarded as dead-end products for some proteins (23) or, alternatively, as by-products acting indirectly as a kind of scaffold that assists secondary nucleation (31). On the other hand, the direct conversion of oligomeric species to mature amyloid fibrils has also been proposed for several proteins such as the amyloid-β peptide (7), β-lactoglobulin (56), insulin (12), and several short amyloidogenic peptides (57), in which oligomers were shown to evolve themselves into amyloidogenic nuclei via direct coil-β conformational conversion (7, 56, 57) or mutual fusion (58). A mechanism has been reported in which oligomers instead of monomers were shown to be involved as a unit of docking for fibril elongation (59). In the present study, the prefibrillar intermediate species have been considered an on-pathway intermediate given the sequential change in the FTIR spectrum and very low amount of residual insulin molecules coexisting with the prefibrillar intermediate (see "Results"); however, it is still difficult to completely rule out the possibility that prefibrillar intermediates are indirectly converted to mature fibrils via monomers produced by the dissociation of intermediates.

Through the present work, we propose that salts are expected to be a useful factor for fine-tuning the energy landscape of protein fibrillation and identifying the stepwise aggregating pathways of amyloid fibrils via a prefibrillar intermediate by the effects of salt will be very profitable for determining the key regions essential for the propagation and cytotoxicity of many amyloidogenic proteins. Although the fibrillation pathway of insulin proteins was investigated under acidic conditions in this study because neutral pH strongly inhibits the amyloid fibril formation through the formation of stable native hexamers (15), it will be important to explore prefibrillar intermediate species at physiological pH and temperature as a future challenge to specify the regions taking a pivotal role in dictating the pathogenesis and transmission of amyloidoses. The molecular design or amino acid substitution targeting those regions will become a promising therapeutic strategy at the molecular level. Furthermore, recognizing the key regions controlling fibril functions further implies the structural bases underlying amyloid polymorphism, and the discovery of different amino acid sequences and/or stereoscopic patterns of side chain docking will improve our understanding of the molecular mechanisms underlying the prion strain phenomenon (55). Intensive studies aimed at such key regions will open a new perspective for the clarification of fibril formation mechanisms, and furthermore, attain a breakthrough for the development of therapeutic strategies against a wide range of amyloidosis and neurodegenerative disorders.

Acknowledgment—We thank Professor Keiko Nishikawa (Graduate School of Advanced Integration Science, Chiba University) for support of x-ray measurements.

REFERENCES

1. Dobson, C. M. (2003) Protein folding and misfolding. *Nature* **426,** 884–890
2. Uversky, V. N., and Fink, A. L. (2004) Conformational constraints for amyloid fibrillation: the importance of being unfolded. *Biochim. Biophys. Acta* **1698,** 131–153
3. Westermark, P., Benson, M. D., Buxbaum, J. N., Cohen, A. S., Frangione, B., Ikeda, S., Masters, C. L., Merlini, G., Saraiva, M. J., and Sipe, J. D. (2007) A primer of amyloid nomenclature. *Amyloid* **14,** 179–183
4. Chiti, F., and Dobson, C. M. (2006) Protein misfolding, functional amyloid, and human disease. *Annu. Rev. Biochem.* **75,** 333–366
5. Wetzel, R. (2006) Kinetics and thermodynamics of amyloid fibril assembly. *Acc. Chem. Res.* **39,** 671–679
6. Kayed, R., Head, E., Thompson, J. L., McIntire, T. M., Milton, S. C., Cotman, C. W., and Glabe, C. G. (2003) Common structure of soluble amyloid oligomers implies common mechanism of pathogenesis. *Science* **300,** 486–489
7. Ahmed, M., Davis, J., Aucoin, D., Sato, T., Ahuja, S., Aimoto, S., Elliott, J. I., Van Nostrand, W. E., and Smith, S. O. (2010) Structural conversion of neurotoxic amyloid-β(1–42) oligomers to fibrils. *Nat. Struct. Mol. Biol.* **17,** 561–567
8. Campioni, S., Mannini, B., Zampagni, M., Pensalfini, A., Parrini, C., Evangelisti, E., Relini, A., Stefani, M., Dobson, C. M., Cecchi, C., and Chiti, F. (2010) A causative link between the structure of aberrant protein oligomers and their toxicity. *Nat. Chem. Biol.* **6,** 140–147
9. Bemporad, F., and Chiti, F. (2012) Protein misfolded oligomers: experimental approaches, mechanism of formation, and structure-toxicity rela-

tionships. *Chem. Biol.* **19,** 315–327
10. Fändrich, M. (2012) Oligomeric intermediates in amyloid formation: structure determination and mechanisms of toxicity. *J. Mol. Biol.* **421,** 427–440
11. Westermark, G. T., and Westermark, P. (2010) Prion-like aggregates: infectious agents in human disease. *Trends Mol. Med.* **16,** 501–507
12. Vestergaard, B., Groenning, M., Roessle, M., Kastrup, J. S., van de Weert, M., Flink, J. M., Frokjaer, S., Gajhede, M., and Svergun, D. I. (2007) A helical structural nucleus is the primary elongating unit of insulin amyloid fibrils. *PLoS Biol.* **5,** e134
13. Oliveira, C. L., Behrens, M. A., Pedersen, J. S., Erlacher, K., and Otzen, D. (2009) A SAXS study of glucagon fibrillation. *J. Mol. Biol.* **387,** 147–161
14. Carulla, N., Zhou, M., Arimon, M., Gairí, M., Giralt, E., Robinson, C. V., and Dobson, C. M. (2009) Experimental characterization of disordered and ordered aggregates populated during the process of amyloid fibril formation. *Proc. Natl. Acad. Sci. U.S.A.* **106,** 7828–7833
15. Groenning, M., Frokjaer, S., and Vestergaard, B. (2009) Formation mechanism of insulin fibrils and structural aspects of the insulin fibrillation process. *Curr. Protein Pept. Sci.* **10,** 509–528
16. Naiki, H., Hashimoto, N., Suzuki, S., Kimura, H., Nakakuki, K., and Gejyo, F. (1997) Establishment of a kinetic model of dialysis-related amyloid fibril extension *in vitro*. *Amyloid* **4,** 223–232
17. Nielsen, L., Khurana, R., Coats, A., Frokjaer, S., Brange, J., Vyas, S., Uversky, V. N., and Fink, A. L. (2001) Effect of environmental factors on the kinetics of insulin fibril formation: elucidation of the molecular mechanism. *Biochemistry* **40,** 6036–6046
18. Brange, J., Andersen, L., Laursen, E. D., Meyn, G., and Rasmussen, E. (1997) Toward understanding insulin fibrillation. *J. Pharm. Sci.* **86,** 517–525
19. Waugh, D. F. (1946) A fibrous modification of insulin. I. The heat precipitate of insulin. *J. Am. Chem. Soc.* **68,** 247–250
20. Whittingham, J. L., Scott, D. J., Chance, K., Wilson, A., Finch, J., Brange, J., and Dodson, G. G. (2002) Insulin at pH 2: structural analysis of the conditions promoting insulin fibre formation. *J. Mol. Biol.* **318,** 479–490
21. Muzaffar, M., and Ahmad, A. (2011) The mechanism of enhanced insulin amyloid fibril formation by NaCl is better explained by a conformational change model. *PLoS One* **6,** e27906
22. Nielsen, L., Frokjaer, S., Carpenter, J. F., and Brange, J. (2001) Studies of the structure of insulin fibrils by Fourier transform infrared (FTIR) spectroscopy and electron microscopy. *J. Pharm. Sci.* **90,** 29–37
23. Grudzielanek, S., Smirnovas, V., and Winter, R. (2006) Solvation-assisted pressure tuning of insulin fibrillation: from novel aggregation pathways to biotechnological applications. *J. Mol. Biol.* **356,** 497–509
24. Kihara, M., Chatani, E., Sakai, M., Hasegawa, K., Naiki, H., and Goto, Y. (2005) Seeding-dependent maturation of β_2-microglobulin amyloid fibrils at neutral pH. *J. Biol. Chem.* **280,** 12012–12018
25. Wu, J. W., Breydo, L., Isas, J. M., Lee, J., Kuznetsov, Y. G., Langen, R., and Glabe, C. (2010) Fibrillar oligomers nucleate the oligomerization of monomeric amyloid β but do not seed fibril formation. *J. Biol. Chem.* **285,** 6071–6079
26. Monti, M., Amoresano, A., Giorgetti, S., Bellotti, V., and Pucci, P. (2005) Limited proteolysis in the investigation of β_2-microglobulin amyloidogenic and fibrillar states. *Biochim. Biophys. Acta* **1753,** 44–50
27. Wilson, L. M., Mok, Y. F., Binger, K. J., Griffin, M. D., Mertens, H. D., Lin, F., Wade, J. D., Gooley, P. R., and Howlett, G. J. (2007) A structural core within apolipoprotein C-II amyloid fibrils identified using hydrogen exchange and proteolysis. *J. Mol. Biol.* **366,** 1639–1651
28. Furukawa, Y., Kaneko, K., Yamanaka, K., and Nukina, N. (2010) Mutation-dependent polymorphism of Cu,Zn-superoxide dismutase aggregates in the familial form of amyotrophic lateral sclerosis. *J. Biol. Chem.* **285,** 22221–22231
29. Tito, P., Nettleton, E. J., and Robinson, C. V. (2000) Dissecting the hydrogen exchange properties of insulin under amyloid fibril forming conditions: a site-specific investigation by mass spectrometry. *J. Mol. Biol.* **303,** 267–278
30. Zhu, Y. F., Lee, K. L., Tang, K., Allman, S. L., Taranenko, N. I., and Chen, C. H. (1995) Revisit of MALDI for small proteins. *Rapid Commun. Mass Spectrom.* **9,** 1315–1320
31. Foderà, V., Cataldo, S., Librizzi, F., Pignataro, B., Spiccia, P., and Leone, M. (2009) Self-organization pathways and spatial heterogeneity in insulin amyloid fibril formation. *J. Phys. Chem. B* **113,** 10830–10837
32. Jansen, R., Dzwolak, W., and Winter, R. (2005) Amyloidogenic self-assembly of insulin aggregates probed by high resolution atomic force microscopy. *Biophys. J.* **88,** 1344–1353
33. Bouchard, M., Zurdo, J., Nettleton, E. J., Dobson, C. M., and Robinson, C. V. (2000) Formation of insulin amyloid fibrils followed by FTIR simultaneously with CD and electron microscopy. *Protein Sci.* **9,** 1960–1967
34. Ahmad, A., Uversky, V. N., Hong, D., and Fink, A. L. (2005) Early events in the fibrillation of monomeric insulin. *J. Biol. Chem.* **280,** 42669–42675
35. Manno, M., Giacomazza, D., Newman, J., Martorana, V., and San Biagio, P. L. (2010) Amyloid gels: precocious appearance of elastic properties during the formation of an insulin fibrillar network. *Langmuir* **26,** 1424–1426
36. Schmit, J. D., Ghosh, K., and Dill, K. (2011) What drives amyloid molecules to assemble into oligomers and fibrils? *Biophys. J.* **100,** 450–458
37. Raman, B., Chatani, E., Kihara, M., Ban, T., Sakai, M., Hasegawa, K., Naiki, H., Rao, C. M., and Goto, Y. (2005) Critical balance of electrostatic and hydrophobic interactions is required for β_2-microglobulin amyloid fibril growth and stability. *Biochemistry* **44,** 1288–1299
38. Yoshimura, Y., Lin, Y., Yagi, H., Lee, Y. H., Kitayama, H., Sakurai, K., So, M., Ogi, H., Naiki, H., and Goto, Y. (2012) Distinguishing crystal-like amyloid fibrils and glass-like amorphous aggregates from their kinetics of formation. *Proc. Natl. Acad. Sci. U.S.A.* **109,** 14446–14451
39. Hong, D. P., Gozu, M., Hasegawa, K., Naiki, H., and Goto, Y. (2002) Conformation of β_2-microglobulin amyloid fibrils analyzed by reduction of the disulfide bond. *J. Biol. Chem.* **277,** 21554–21560
40. Relini, A., Torrassa, S., Ferrando, R., Rolandi, R., Campioni, S., Chiti, F., and Gliozzi, A. (2010) Detection of populations of amyloid-like protofibrils with different physical properties. *Biophys. J.* **98,** 1277–1284
41. Chimon, S., and Ishii, Y. (2005) Capturing intermediate structures of Alzheimer's β-amyloid, Aβ(1–40), by solid-state NMR spectroscopy. *J. Am. Chem. Soc.* **127,** 13472–13473
42. Bocharova, O. V., Makarava, N., Breydo, L., Anderson, M., Salnikov, V. V., and Baskakov, I. V. (2006) Annealing prion protein amyloid fibrils at high temperature results in extension of a proteinase K-resistant core. *J. Biol. Chem.* **281,** 2373–2379
43. Esler, W. P., Stimson, E. R., Jennings, J. M., Vinters, H. V., Ghilardi, J. R., Lee, J. P., Mantyh, P. W., and Maggio, J. E. (2000) Alzheimer's disease amyloid propagation by a template-dependent dock-lock mechanism. *Biochemistry* **39,** 6288–6295
44. Reddy, G., Straub, J. E., and Thirumalai, D. (2009) Dynamics of locking of peptides onto growing amyloid fibrils. *Proc. Natl. Acad. Sci. U.S.A.* **106,** 11948–11953
45. Chatani, E., Ohnishi, R., Konuma, T., Sakurai, K., Naiki, H., and Goto, Y. (2010) Pre-steady-state kinetic analysis of the elongation of amyloid fibrils of β_2-microglobulin with tryptophan mutagenesis. *J. Mol. Biol.* **400,** 1057–1066
46. Konuma, T., Chatani, E., Yagi, M., Sakurai, K., Ikegami, T., Naiki, H., and Goto, Y. (2011) Kinetic intermediates of β_2-microglobulin fibril elongation probed by pulse-labeling H/D exchange combined with NMR analysis. *J. Mol. Biol.* **405,** 851–862
47. Yanagi, K., Sakurai, K., Yoshimura, Y., Konuma, T., Lee, Y. H., Sugase, K., Ikegami, T., Naiki, H., and Goto, Y. (2012) The monomer-seed interaction mechanism in the formation of the β_2-microglobulin amyloid fibril clarified by solution NMR techniques. *J. Mol. Biol.* **422,** 390–402
48. Ivanova, M. I., Thompson, M. J., and Eisenberg, D. (2006) A systematic screen of β_2-microglobulin and insulin for amyloid-like segments. *Proc. Natl. Acad. Sci. U.S.A.* **103,** 4079–4082
49. Sawaya, M. R., Sambashivan, S., Nelson, R., Ivanova, M. I., Sievers, S. A., Apostol, M. I., Thompson, M. J., Balbirnie, M., Wiltzius, J. J., McFarlane, H. T., Madsen, A. Ø., Riekel, C., and Eisenberg, D. (2007) Atomic structures of amyloid cross-β spines reveal varied steric zippers. *Nature* **447,** 453–457
50. Goldschmidt, L., Teng, P. K., Riek, R., and Eisenberg, D. (2010) Identifying the amylome, proteins capable of forming amyloid-like fibrils. *Proc. Natl. Acad. Sci. U.S.A.* **107,** 3487–3492

51. Ivanova, M. I., Sievers, S. A., Sawaya, M. R., Wall, J. S., and Eisenberg, D. (2009) Molecular basis for insulin fibril assembly. *Proc. Natl. Acad. Sci. U.S.A.* **106,** 18990–18995
52. Sievers, S. A., Karanicolas, J., Chang, H. W., Zhao, A., Jiang, L., Zirafi, O., Stevens, J. T., Münch, J., Baker, D., and Eisenberg, D. (2011) Structure-based design of non-natural amino-acid inhibitors of amyloid fibril formation. *Nature* **475,** 96–100
53. Shen, Y., Joachimiak, A., Rosner, M. R., and Tang, W. J. (2006) Structures of human insulin-degrading enzyme reveal a new substrate recognition mechanism. *Nature* **443,** 870–874
54. Jiménez, J. L., Nettleton, E. J., Bouchard, M., Robinson, C. V., Dobson, C. M., and Saibil, H. R. (2002) The protofilament structure of insulin amyloid fibrils. *Proc. Natl. Acad. Sci. U.S.A.* **99,** 9196–9201
55. Ohhashi, Y., Ito, K., Toyama, B. H., Weissman, J. S., and Tanaka, M. (2010) Differences in prion strain conformations result from non-native interactions in a nucleus. *Nat. Chem. Biol.* **6,** 225–230
56. He, X., Giurleo, J. T., and Talaga, D. S. (2010) Role of small oligomers on the amyloidogenic aggregation free-energy landscape. *J. Mol. Biol.* **395,** 134–154
57. Bleiholder, C., Dupuis, N. F., Wyttenbach, T., and Bowers, M. T. (2011) Ion mobility-mass spectrometry reveals a conformational conversion from random assembly to β-sheet in amyloid fibril formation. *Nat. Chem.* **3,** 172–177
58. Hill, S. E., Robinson, J., Matthews, G., and Muschol, M. (2009) Amyloid protofibrils of lysozyme nucleate and grow via oligomer fusion. *Biophys. J.* **96,** 3781–3790
59. Serio, T. R., Cashikar, A. G., Kowal, A. S., Sawicki, G. J., Moslehi, J. J., Serpell, L., Arnsdorf, M. F., and Lindquist, S. L. (2000) Nucleated conformational conversion and the replication of conformational information by a prion determinant. *Science* **289,** 1317–1321